Asymmetry Measurements in the Scattering of 155-Mev Neutrons by Carbon, Aluminum, Copper, Cadmium, and Lead*

R. S. HARDING†
University of Rochester, Rochester, New York
(Received March 12, 1958)

The asymmetry in the scattering of a 13% polarized (155±5)-Mev neutron beam from C, Al, Cu, Cd, and Pb was measured at angles below the first maximum in the asymmetry. The scattered neutrons were detected by a large volume scintillator with an energy threshold determined by pulse-height discrimination. Optical-model calculations were performed by a WKB phase-shift analysis to find the "best fit" to the 155-Mev proton-carbon polarization data from Uppsala. The nuclear parameters determined in this manner were then used to calculate the polarization and the cross sections by WKB and Born approximations for comparison with the data of this experiment. The neutron polarization and the qualitative behavior of the neutron differential cross sections were well explained by the model, but sizable discrepancies were found between the predicted and measured absolute cross sections.

INTRODUCTION

THERE has been considerable interest in recent years in the experimental and theoretical aspects of the scattering of polarized nucleons by complex nuclei.[1] The most recent experiments with polarized protons have been of sufficient precision to furnish a severe test of the optical model. Hafner[2] has shown that a good fit can be obtained to the polarization angular distributions in four elements of widely different atomic number if one takes a nuclear model employing an attractive complex potential with an inverted spin-orbit term. The model should also explain neutron scattering data. However, the experimental situation in neutron scattering is much less advanced because of greater technical difficulties. The majority of the published data on the scattering of polarized neutrons are those of Siegel,[3] who used a beam of mean energy 350 Mev. We therefore felt that additional measurements, particularly at an energy coinciding with that at which proton polarization data exists, would be of value in providing a further test of the nuclear model.

We discuss here some measurements of the scattering of 155-Mev partially polarized neutrons by carbon, aluminum, copper, cadmium, and lead. In this, as in most other neutron scattering experiments, it was not possible to achieve a clear separation of elastic and inelastic scattering events. This is because the primary neutron energy spectrum is very broad, and the neutron detection method provides little energy resolution. Since the model calculations apply only to elastic scattering, we have confined measurements to the small-angle region, where the scattering is expected to be predominantly elastic. The data are compared with WKB and Born approximation calculations of the polarization, using a model which accounts satisfactorily for the 155-Mev polarized proton scattering data from Uppsala.[4]

APPARATUS

The experimental layout is illustrated in Fig. 1. The neutron beams used in this experiment were derived from three beryllium and two carbon targets inside the University of Rochester 130-in. synchrocyclotron. The targets and the axis of the collimating system were aligned optically to provide neutron beams at 0° and ±20° 43 sec with respect to the internal proton beam. The targets hereafter will be referred to as follows: numbers 3, 4, 5, and 6 as +C, +Be, −C, and −Be, respectively, and number 13 as 0° Be. The neutron spectrum from the +Be target was measured, at the second scattering position, by examining the differential range spectrum of recoil protons from *n-p* collisions. The neutron spectrum was peaked at 168 Mev and had a full width at half-maximum of 80 Mev. The so-called effective neutron spectrum, obtained by folding a calculated neutron detection efficiency and the measured neutron spectrum, gave a full width at half-maximum of approximately 60 Mev for a 100 Mev counter threshold.

A neutron monitor consisting of a triple scintillation counter telescope and a CH_2 converter was located at the channel exit in the north shielding car. Copper absorbers were placed in the recoil proton telescope to restrict the response to the higher energy components of the neutron beam. Two neutron counters were used in different portions of this experiment to detect the high-energy neutrons. A large counter, consisting of a plastic scintillator $16\frac{1}{2}$ in. long and 3.6 in. in diameter, was used for many of the measurements on carbon and aluminum. This piece of scintillator was made by polymerizing vinyl-toluene monomer containing: 2.5%,

* Research supported by the U. S. Atomic Energy Commission.
† Now at Combustion Engineering Inc., Windsor, Connecticut. This report constitutes a part of the author's Ph.D. thesis, Atomic Energy Commission Report NYO-8056 (unpublished).
[1] An excellent bibliography of most of the experimental and theoretical work in this field is found in the review article by L. Wolfenstein, in *Annual Review of Nuclear Science* (Annual Reviews, Inc., Stanford, 1956), Vol. 6, p. 43.
[2] E. M. Hafner, Phys. Rev. **111**, 297 (1958).
[3] R. T. Siegel, Phys. Rev. **100**, 437 (1955).
[4] Alphonce, Johansson, and Tibell, Nuclear Phys. (to be published).

by weight, p terphenyl as an activator; 0.02%, by weight, 1,1,4,4-tetraphenylbutadiene as a wavelength shifter; and 0.01%, by weight, zinc sterarate as a releasing agent from the glass mold. A small counter, consisting of a piece of commercial Sintilon[5] 1 in. wide, 3 in. high, and 10 in. long, was used for the measurements on copper, cadmium, lead, and also for the measurements on carbon and aluminum at the smaller angles.

Each counter was viewed by a single RCA 14-stage photomultiplier. The best operation, under the conditions of this experiment, was obtained with the developmental model RCA-C7187A. A 2-in. thick copper absorber was placed before each neutron counter to degrade the energy of the most energetic protons to a value below the detection threshold. Long-term thermal fluctuations were minimized by a thermistor-controlled heating arrangement which passed air into thin Styrofoam shields surrounding each counter. The photomultiplier high voltage was monitored by a Leeds and Northrup type K potentiometer and controlled to within ± 0.2 volt out of 1840 volts.

Operation of the 14-stage photomultiplier into a 160-ohm load provided sufficient pulse height for direct fast pulse-height discrimination. Two discriminators were used in this experiment. The first contained three integral channels set to provide data at threshold energies of 100, 110, and 125 Mev. The second discriminator contained one integral channel. This discriminator employed different circuitry and was used to check the three-channel discriminator for possible counting errors.

EXPERIMENTAL PROCEDURE

The neutron counters were calibrated for pulse height *versus* energy loss in the external proton beam. Neutron beam profiles were measured, at reduced beam levels, for the 0° Be and $\pm$Be targets to determine the effective center of the neutron beams. The zero angle was taken as the mean of the effective beam centers from the pulse and minus first scattering targets. This choice of zero angle introduces an angular error which, by coincidence, always increases the asymmetry from each first scattering target. When measuring asymmetries the cyclotron oscillator was turned off as the counter was moved through the zero-angle position, since noticeable pulse-height shifts were observed after the neutron counter had been subjected to the full-intensity direct neutron beam. The background rates were measured by displacing the second scattering target far enough from the second scattering center so that slit-edge scattered neutrons were not attenuated by the targets.

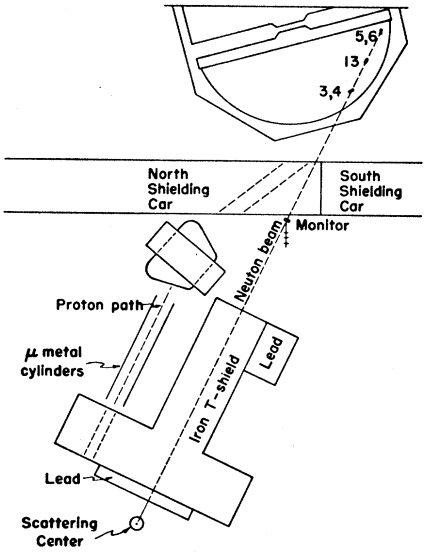

FIG. 1. Floor plan of experimental layout.

RESULTS

The asymmetries were calculated in the standard manner, and were taken to be positive when the direction of the more intense scattered beam was the same as the first p-n scattering. The asymmetries from the plus and minus first scattering targets were combined and then corrected for the angular error introduced by our choice of zero angle. The correction factor was evaluated by the following equation:

$$\delta\epsilon = \tfrac{1}{2}[\,|\Delta R/R| + |\Delta L/L|\,],$$

where $\Delta R/R$ and $\Delta L/L$ represent the percentage change in counting rate per unit change in the second scattering angle. These quantities were evaluated from the relative angular distribution of the second target

TABLE I. Corrected asymmetry data.

Lab angle	C	Lab angle	Al	Lab angle	Cu	Lab angle	Cd	Lab angle	Pb
3½°	0.030±0.009	3½°	0.025±0.005	2°	0.002±0.009	3½°	0.012±0.007	1½°	−0.002±0.009
5°	0.035±0.011	5°	0.027±0.005	3½°	0.027±0.004	6½°	0.057±0.007	2°	0.004±0.008
7½°	0.046±0.008	7°	0.060±0.009	5°	0.039±0.006	9½°	0.077±0.014	3½°	0.014±0.004
10°	0.077±0.011	7½°	0.070±0.012	6½°	0.050±0.004			5°	0.041±0.005
12½°	0.084±0.011	10°	0.083±0.010	8°	0.070±0.005			6½°	0.055±0.006
15°	0.111±0.010	12½°	0.080±0.012	9½°	0.076±0.006			8°	0.078±0.006
20°	0.136±0.023	15°	0.0128±0.012	11°	0.089±0.011			9½°	0.069±0.010
25°	0.055±0.025	20°	0.089±0.019						

[5] Product of National Radiac, Newark, New Jersey.

TABLE II. Unpolarized differential cross sections (barns/sterad).

Lab angle	C	Lab angle	Al	Lab angle	Cu	Lab angle	Cd	Lab angle	Pb
3½°	1.07±0.08	3½°	3.59±0.24	3½°	12.1±0.8	3½°	23.9±1.7	3½°	49.2±3.3
5°	1.03±0.08	5°	3.16±0.21	5°	8.79±0.59	6½°	9.80±0.65	5°	27.8±1.9
7½°	0.76±0.05	7°	2.32±0.17	6½°	6.42±0.43	9½°	2.45±0.17	6½°	13.3±0.9
10°	0.56±0.04	7½°	2.05±0.14	8°	3.90±0.26			8°	4.77±0.32
12½°	0.35±0.03	10°	1.23±0.09	9½°	2.32±0.16			9½°	1.91±0.13
15°	0.21±0.02	12½°	0.59±0.04	11°	1.23±0.08				
20°	0.075±0.006	15°	0.28±0.02						
25°	0.034±0.003	20°	0.081±0.006						

yields. The asymmetries calculated from the 100-Mev threshold data are tabulated in Table I. The data from the 110- and 125-Mev threshold channels were indistinguishable from the 100-Mev data.

The relative yields *versus* angle for the various second scatterers were corrected for multiple scattering and attenuation after the method of Bratenahl.[6] An additional correction was made for the attenuation of the slit-edge scattered neutrons due to the second scattering target when the latter was in the second scattering position. The effective center of the neutron counter was calculated from the variation of the counting rate with displacement of the counter from the second scattering center at fixed angle. The effective area of illumination of the target was calculated from the geometry of the collimation system and the full width at half-maximum of the neutron beam distribution at the second scattering center. Thus the absolute differential cross sections could be calculated from the ratio of the counting rate per unit monitor in the direct and scattering beams. The cross sections are tabulated in Table II.

The effective energy of the polarized neutron beam was measured by a carbon attenuation experiment in good geometry. The total cross section was found to be 327±2 mb which corresponds to an effective energy of 155±5 Mev according to the published experimental data[7] on the *n*-carbon total cross section.[8]

A value for the polarization of the primary polarized neutron beam was deduced in the following manner. The asymmetry was measured for the processes represented by *p*-C-*n*-C-*p* and *p*-Be-*n*-C-*p*. Neglecting the energy difference between the first and second scattering and assuming that the asymmetry is equal to the product of P_1 and P_2 for the charge exchange scatterings, we obtain the following result for a 98-Mev threshold of proton detection:

$$P_{\mathrm{Be}}=\epsilon_{\mathrm{Be,C}}/(\epsilon_{\mathrm{C,C}})^{\frac{1}{2}}=0.130\pm0.013.$$

By use of the foregoing value for P_{Be} and the asymmetries of Table I, the polarizations plotted in Figs. 4(a) through (e) were calculated for the various second-scattering targets.

ANALYSIS

In this analysis, we examine the WKB optical-model calculations of the polarization and cross section using a nuclear model consisting of an inverted spin-orbit potential in addition to an attractive, complex central potential with a Woods and Saxon[9] type of radial distribution. In particular, we wish to determine what restrictions are placed on the nuclear parameters if we require a reasonable fit to the 155-Mev proton polarization data from Uppsala.[4] The nuclear parameters determined in this manner are then used to calculate the polarization in neutron scattering; the predictions are to be compared with the results of this experiment under the assumption that the nuclear radius is proportional to $A^{\frac{1}{3}}$.

The nuclear potential was taken to be

$$V_1^{+}=\left[-(u+iv)+\mu g^2\frac{1}{r}\frac{d}{dr}\right]\rho(r) \quad \text{for } j=1+\tfrac{1}{2},$$

$$V_1^{-}=\left[-(u+iv)-\mu g^2\frac{l+1}{r}\frac{d}{dr}\right]\rho(r) \quad \text{for } j=1-\tfrac{1}{2},$$

where u, v, and μ are real positive quantities expressed in Mev, g is a length, and m is the mass of the incident nucleon. The function $\rho(r)$ is equal to $[1+e^{(r-r_0)/a}]^{-1}$, where r_0 is proportional to $A^{\frac{1}{3}}$ and a is a measure of the surface thickness of the nuclear force. The nuclear phase shifts, $\delta_{lN}^{\pm}$, corresponding to these potentials, were computed in the WKB approximation.[10] The modified Coulomb phase shifts, δ_{lC}, corresponding to the case of a uniformly charged sphere of radius r_1, were calculated by the equations of Gatha and Riddell.[11] The total phase shift for the scattering of protons is then represented by the equation

$$\delta_l^{\pm}=\delta_{l,n}^{\pm}+\delta_{l,C}.$$

The equations for the scattering matrix, WKB scatter-

[6] A. Bratenahl *et al.*, Phys. Rev. **77**, 597 (1950).
[7] A. E. Taylor and E. Wood, Phil. Mag. **44**, 1995 (1953).
[8] This value of the effective energy is significantly lower than the peak of the neutron spectrum; this effect is a result of the increasing carbon total cross section with decreasing neutron energy which lowers the effective energy for scattering.
[9] R. D. Woods and D. S. Saxon, Phys. Rev. **95**, 577 (1954).
[10] N. F. Mott and H. S. W. Massey, *Theory of Atomic Collisions* (Clarendon Press, Oxford, 1949), second edition.
[11] K. M. Gatha and R. J. Riddell, Phys. Rev. **86**, 1035 (1952).

ing amplitudes, polarization, and cross sections are the same as those of Sternheimer.[12]

The WKB calculations were performed on an IBM-650 computer, at the University of Rochester computing center, using the Bliss interpretive system. A number of calculations were made for the scattering of neutrons and protons by carbon to study the behavior of the polarization and cross section for variations of the optical parameters,[13] k_1 and K; the coefficient of the spin-orbit term, μg^2; the charge radius, r_1; and the parameters governing the radial distribution of the nuclear potential, r_0 and a. In view of the number of parameters involved, we found it convenient to use a parameter[14] A, defined as the ratio of the coefficient of the spin-orbit term to the magnitude of the central potential, to establish a correspondence with the equation for the polarization, $P(\theta)$, in Born approximation. For our choice of potentials, A is expressed by the following equation:

$$A=\frac{k}{E}\left(\frac{\mu g^2}{(2k_1)^2+K^2}\right),$$

where k and E are the wave number and total energy, respectively, of the incident nucleon in the center-of-mass system. We shall summarize certain characteristic trends which were observed in our more or less random variation of the parameters.

(1) Increasing the charge radius from 2.5 to 3.1 fermis (1 fermi$\equiv 10^{-13}$ cm) had a negligible effect on the polarization of protons scattered by carbon.

(2) The position of the first minimum in the polarization and the first minimum of the unpolarized cross section depend on

(a) the shape parameters, r_0 and a;

(b) the magnitude of the coefficient of the spin-orbit term, μg^2: increasing μg^2, with the remainder of the parameters unchanged, displaces the minimum to a smaller angle;

(c) the magnitude of the absorption coefficient K: increasing K alone displaces the minimum to a larger angle.

(3) The height of the first maximum in the polarization varies as follows:

(a) For $k_1=0$, $P_{\max}$ approaches 1.

(b) For nonzero values of k_1 and small a, decreasing the parameter A decreases $P_{\max}$ and the rate of rise of the polarization with angle. This latter observation is consistent with a Born approximation calculation.

(4) The position and magnitude of $P_{\max}$ remains constant over a limited range of r_0 and a, for fixed values of $K/(2k_1)$ and the parameter A, in qualitative agreement with Born approximation predictions of the polarization.

(5) The total elastic and forward differential cross section increase as K and μg^2 increase and are not significantly dependent on k_1.

(6) For a given nuclear size, $P(\theta)$ in neutron scattering remains unchanged when the potential strengths are increased in such a manner as to keep the magnitudes of $K/(2k_1)$ and A constant. The total elastic and inelastic cross sections increase, the former increasing at a faster rate per unit change in K than the latter. We find that in order to obtain a reasonable elastic cross section, the inelastic cross section is consistently underestimated by approximately 30% for the "best fit" to the 155-Mev proton-carbon polarization data.

(7) Decreasing the value of a concentrates the spin-orbit potential at the nuclear surface and leads to a narrow first maximum in the polarization. The "best fit" to the 155-Mev proton-carbon polarization data is obtained for values of a of the order of 0.1 fermi.

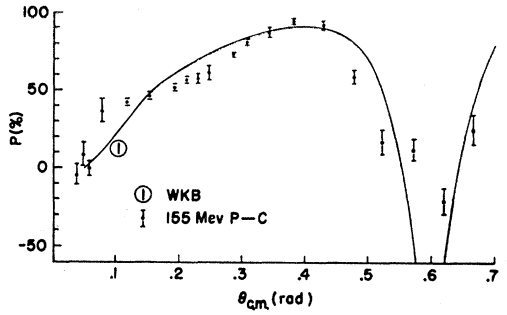

FIG. 2. WKB proton polarization *versus* angle for carbon and experimental data at 155 Mev (reference 7).

In Fig. 2 a comparison is made between the 155-Mev proton-carbon polarization data from Uppsala and a WKB calculation based on the following parameters:

$$2k_1=2.145\times10^{12}\ \text{cm}^{-1}, \qquad a=0.1\ \text{fermi},$$
$$K=4.31\times10^{12}\ \text{cm}^{-1}, \qquad r_0=2.53\ \text{fermis},$$
$$\mu g^2=1.59\times10^{-25}\ \text{Mev-cm}^2, \qquad r_1=3.1\ \text{fermis}.$$

Figure 3 is a comparison between the Uppsala 155-Mev proton-copper polarization data and a WKB calculation using the same values of k_1, K, μg^2, and a. The values of r_0 and r_1 were taken as 4.4 fermis for copper. The calculated value of K, based on the equations of Cassels and Lawson,[15] is 4.1×10^{12} cm^{-1}; this value of K would probably give as good a fit to the polarization data as the value stated above. In Figs. 4(a) through (e), the neutron polarization data of this experiment are compared with calculations of the following types:

[12] R. M. Sternheimer, Phys. Rev. **97**, 1314 (1955).
[13] Fernbach, Serber, and Taylor, Phys. Rev. **75**, 1352 (1949).
[14] I. I. Levintov, Doklady Akad. Nauk. S.S.S.R. **107**, 240 (1956); translation in Soviet Phys. Doklady **1**, 175 (1956).
[15] J. M. Cassels and J D. Lawson, Proc. Phys. Soc. (London) **A67**, 125 (1954).

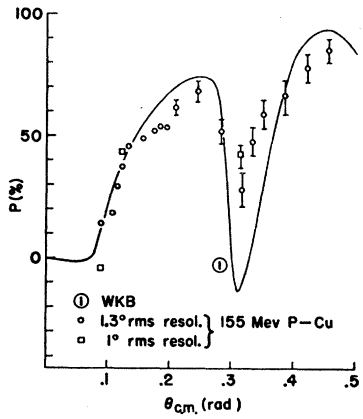

FIG. 3. WKB proton polarization *versus* angle for copper and experimental data at 155 Mev (reference 7).

(1) the WKB prediction of $P(\theta)$ which, for neutrons, considers no electromagnetic interactions;

(2) the Born approximation prediction of $P(\theta)$ for pure nuclear scattering;

(3) the Born approximation prediction for $P(\theta)$ in which the nuclear scattering amplitudes were combined with the scattering amplitudes for the interaction of the neutron magnetic moment with the Coulomb field.

The Born approximation calculations were carried out for the case of a square well of radius r_0; the central potentials and the coefficient of the spin-orbit term were of the same magnitude as in the WKB calculations. The cross sections based on the WKB and Born approximation calculations are summarized in Table III.

TABLE III. Comparison of calculated and experimental cross sections for scattering of 155-Mev neutrons.

	C	Al	Cu	Cd	Pb
Total cross sections in mb:					
σ_t (WKB)[a]	260	511	1014	1573	2546
σ_t (WKB)[b]	293	538	1077	1667	2664
σ_t (BA)[b]	274	611	1426	2541	4675
σ_t (exp)[c]	330±3	677±11	1376±18	2200	3499±26
Inelastic cross sections in mb:					
σ_a (WKB)	153	288	546	825	1285
σ_a (exp)[d]	221±10	418±14	741±13	1073±19	1704±24
Elastic cross sections in mb:					
σ_e (WKB)	107	223	468	748	1261
σ_e (exp)[e]	109±13	259±25	635±31	1127	1795±50
Forward differential cross sections in barns/steradian:					
$\sigma_0°$ (WKB)	0.385	1.41	5.90	15	38
$\sigma_0°$ (BA)	0.398	2.19	12.5	40.6	138
$\sigma_0°$ (exp)[f]	1.19±0.06	4.15±20	14.6±0.5	33.0±1.4	73.1±3.2

[a] Sum of σ_e(WKB) and σ_a (WKB).
[b] Calculated from optical theorem: $\sigma_t = (4\pi/k)\,\mathrm{Im}f(0°)$.
[c] See reference 7.
[d] R. G. P. Voss and R. Wilson, Proc. Roy. Soc. (London) **A236**, 41 (1956).
[e] σ_t (exp) $-\sigma_a$ (exp).
[f] Van Zyl, Voss, and Wilson, Phil. Mag. 1, 1003 (1956).

DISCUSSION

A set of nuclear parameters were found which provide a reasonable fit to the 155-Mev proton-carbon data from Uppsala. When the nuclear radius is extrapolated to copper, using a $A^{\frac{1}{3}}$ dependence, the same nuclear parameters also give reasonable agreement with the 155-Mev proton-copper polarization from Uppsala. Neutron polarization curves were calculated by the WKB method (Woods and Saxon radial distribution) and Born approximation (square well) with the same nuclear parameters for comparison with the results of this experiment. The Born approximation and WKB predictions for $P(\theta)$, with neglect of electromagnetic interactions, are quite similar in the small-angle region. This observation is in agreement with Levintov's[14] small-angle approximation of the WKB calculation of the polarization. The experimental neutron data for the heavy elements indicate a reversal of the sign of the polarization at small angles which is consistent with out knowledge of the polarization resulting from the interaction of the neutron magnetic moment with the nuclear Coulomb field. The phase shifts resulting from this interaction are small; therefore no attempt was made to include the interaction in the WKB calculation. The Born-approximation scattering amplitudes for the neutron magnetic moment interaction were added to the Born-approximation nuclear scattering amplitudes and the polarization computed. The resulting curves are in good agreement with the neutron polarization data in the heavy elements.

The data of this experiment would be consistent with a displacement of $P_{\max}$ to a smaller angle. On the basis of the observations described earlier, this could be accomplished by increasing the ratio of spin-orbit potential to central potential, or by increasing the nuclear radius. The qualitative behavior of the WKB unpolarized differential cross sections for neutrons and protons on carbon is consistent with experimental data, although the diffraction minima are not as prominent experimentally. Their diminution may be attributed to the poor angular resolution of the detecting apparatus and to contamination by inelastic scattering events. Quantitative comparison between the calculated cross sections and experimental data discloses certain obvious discrepancies. The forward WKB differential cross sections are consistently low by a factor of two or three whereas those calculated by Born approximation start low at carbon and cross over the experimental data between copper and cadmium. The integrated WKB elastic cross sections rapidly decrease below the experimental values with increasing atomic weight and the inelastic cross sections are underestimated by 30% for all elements. The absorption coefficient, K, may be calculated in terms of the particle density in nuclear matter times the cross section for scattering of neutrons by the nucleons using the equations of Cassels and Lawson. In order to obtain agreement between the calculated and experimental absorption cross sections using the calculated value of K, the value of r_0, for $a=0.1$ fermi, is of the order of $1.4A^{\frac{1}{3}}$ fermis. This radius would give obvious disagreement between the WKB calculation of $P(\theta)$ and the experimental data in the region of the first minimum of the polarization.

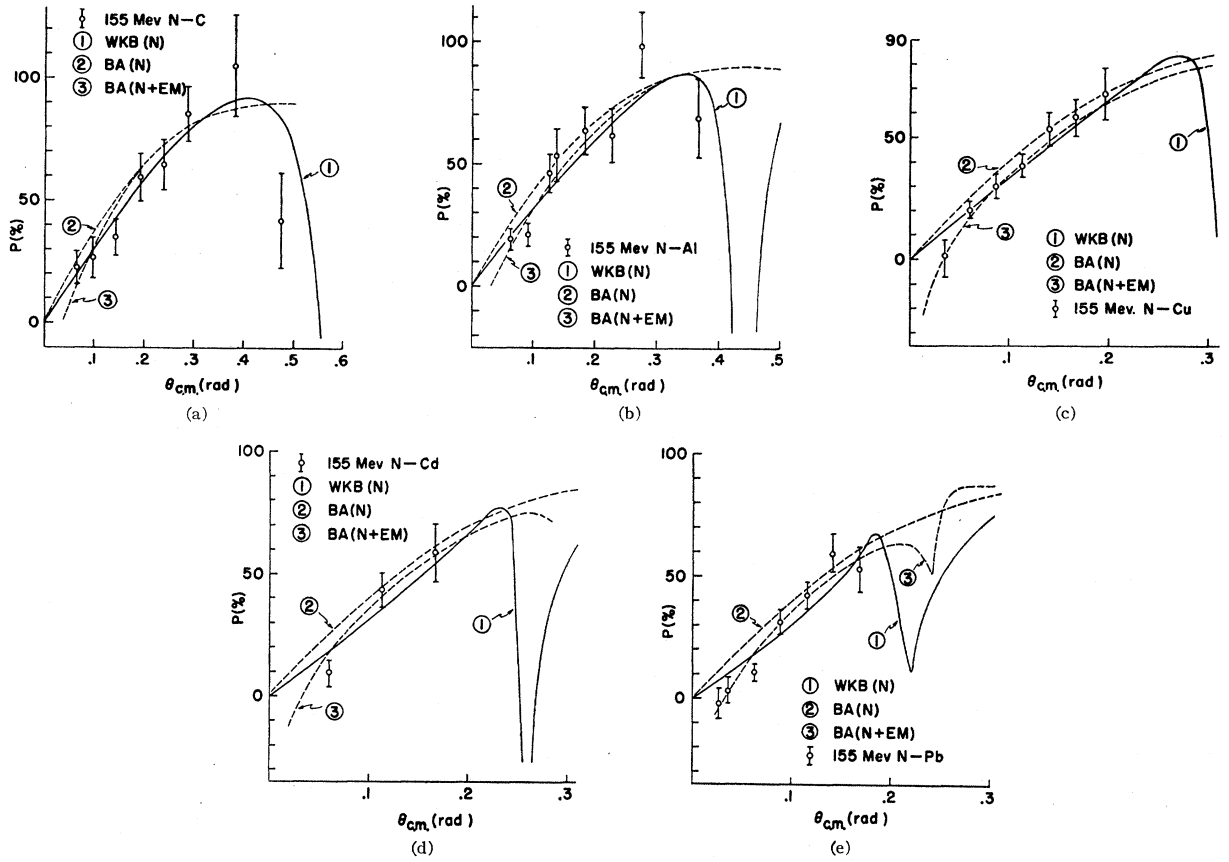

FIG. 4. WKB and Born approximation neutron polarization *versus* angle and data of this experiment. The symbols (N) and $(N+EM)$ refer to nuclear and nuclear plus electromagnetic.

The quantitative behavior of the WKB cross sections indicates an underestimate of the nuclear size for our choice of potentials. An increase of the nuclear size would affect the position of the minimum in $P(\theta)$, but it is not obvious that it would also affect the position of the maximum since the position of the latter was found to be dependent only on the relative magnitudes of the potentials over a limited range of the nuclear size. With the present form of the IBM calculation program, it was not feasible to make a systematic search for a set of nuclear parameters which would provide reasonable agreement between the nuclear cross sections and the polarization data obtained in this experiment.

There are various points of view as to where the discrepancies may arise in these calculations. The fault may lie in the form of the potential, the method of calculation, or both. The WKB method of calculating phase shifts is approximate and the only valid test of the method is a comparison with an exact calculation. Since we have not performed the exact calculations, we can only conclude that a WKB phase-shift analysis for a real, inverted spin-orbit potential in addition to a complex central potential does not provide quantitative agreement with experimental cross-section data when the nuclear parameters are determined by a "best fit" to the large-angle polarization at 155 Mev.

ACKNOWLEDGMENTS

The author wishes to express his sincere appreciation to Professor J. Tinlot for supervising this work, and to Professor E. Hafner for valuable help in performing the calculations on the IBM computer. The assistance of Professor A. Roberts, Dr. E. Heer, Mr. K. Gotow, and Mr. E. Garelick is gratefully acknowledged.